Chemical Science

ROYAL SOCIETY OF CHEMISTRY

EDGE ARTICLE

View Article Online
View Journal

Cite this: DOI: 10.1039/d5sc05666g

All publication charges for this article have been paid for by the Royal Society of Chemistry

Structural and reactivity investigations using organo-copper(I) and zinc(II) complexes with hydrogen and carbon dioxide†

Bradley E. Cowie, [a] Andreas Phanopoulos,[ab] Milo S. P. Shaffer *[cd] and Charlotte K. Williams *[a]

Heterogeneous copper zinc catalysts are widely used in syn-gas or carbon dioxide hydrogenation to methanol, but the structures and reactivity at the catalytic active sites are still not fully understood. Well-defined metal complexes and clusters may help reveal the structures of key intermediates, including for catalytic reactions involving gaseous species. Here, a tri-copper(I) complex, $[Cu_3\{\mu{:}\kappa^3(PPC)\text{-dppm}'\}_2\{\mu{:}\kappa^2(PP)\text{-dppm}'\}]$ **1** (dppm′ = $[(Ph_2P)_2CH]^-$) is used as the starting point to investigate reactivity with hydrogen and carbon dioxide in solution and at low temperatures (20–60 °C) and gas pressures (1 bar or lower). Complex **1** reacts with hydrogen to afford a copper-hydride cluster, $[Cu_5(\mu\text{-H})(\mu_3\text{-H})_2(\mu{:}\kappa^3(PPC)\text{-dppm}')_2(\mu{:}\kappa^2(PP)\text{-dppm})_2]$ **2**, which contains five Cu^I centres and three hydrido ligands. The reaction of **2** with carbon dioxide provides a tri-copper(I)-bis(formate)(hydrido) complex, $[Cu_3(\mu_3\text{-H})(\kappa^1(O)\text{-}O_2CH)(\mu{:}\kappa^2(OO)\text{-}O_2CH)(\mu{:}\kappa^2(PP)\text{-dppm})_3]$ **3**, in which two molecules of carbon dioxide react with the hydrides to produce formate ligands. Treating **1** with an organozinc(II) complex, $[Zn(C_6F_5)_2]$, affords a hetero-tetrametallic $Cu^I_2Zn^{II}_2$ complex, $[Cu_2(\mu{:}\kappa^3(PPC)\text{-dppm}')_2\{Zn(C_6F_5)_2\}_2]$ **4**. Complex **4** features two cationic Cu(I) and two anionic Zn(II) centres, adopting an unusual copper zincate speciation, and reacts with carbon dioxide to form a bis(carboxylate)-$Cu^I_2Zn^{II}_2$ complex, $[Cu_2(\mu{:}\kappa^4(PPOO)\text{-dppm}'')_2\{Zn(C_6F_5)_2\}_2]$ **5**; carbon dioxide inserts into the Zn–C bond and forms a new C–C bond with the methine carbon of the dppm′ ligand. Overall, the structures and reactivity indicate that Cu^I sites readily form hydrides, on exposure to hydrogen; these cuprous hydrides react with CO_2 to produce formate, and cuprous zincates react with CO_2 to afford carboxylates.

Received 28th July 2025
Accepted 4th November 2025

DOI: 10.1039/d5sc05666g

rsc.li/chemical-science

Introduction

The hydrogenation of carbon dioxide (CO_2) to form methanol is important for the production of sustainable liquid transport fuels and energy vectors.[1] To limit the resulting greenhouse gas emissions, the hydrogen should be renewably sourced, *e.g.* by solar powered water electrolysis.[2–4] Currently, methanol is industrially produced on a 100 Mt per annum scale from synthesis gas *via* hydrogenation of both CO and CO_2, with the key reactions involving both direct hydrogenations of these carbon oxides and exchange between them by the reverse water–gas shift reaction.[5,6] The syn-gas to methanol reactions operate at high temperatures (250 °C) and pressures (>50 bar) using heterogeneous $Cu/ZnO/Al_2O_3$ catalysts.[7] Computational[8] and isotopic-labelling studies[9] have revealed that, in syn-gas transformations, most of the methanol produced originates from the hydrogenation of CO_2, with CO playing a key role in the catalytic cycle through reactions with surface-oxygen atoms originating from water production, as well as participating in CO-assisted hydrogenation of surface intermediates.[8,10,11] Direct CO_2 hydrogenation is also feasible using the same Cu/ZnO catalysts and, once again, low temperature reactions are desirable to drive equilibria.[12] In both reactions, there is considerable debate regarding the catalyst active sites, including different hypotheses regarding metal oxidation states, structures, speciation, and mechanisms/functions; there is general consensus that active sites occur at interfaces between copper(0/I) and zinc(0/II) surfaces.[5,6,10,12–24] There are many approaches to exploring this complex catalytic problem; this work focusses on using well-defined copper and zinc complexes to better understand reactivity with hydrogen and carbon dioxide.

Homogeneous copper or copper–zinc catalysts are not yet known for CO_2 hydrogenation to methanol, but well-defined complexes or clusters may be useful to investigate key

[a]Department of Chemistry, University of Oxford, Chemistry Research Laboratory, 12 Mansfield Road, Oxford, OX1 3TA, UK. E-mail: charlotte.williams@chem.ox.ac.uk
[b]Department of Chemistry, University of Bath, Claverton Down, Bath, BA2 7AX, UK
[c]Department of Chemistry, Imperial College London, 82 Wood Lane, London, W12 0BZ, UK. E-mail: m.shaffer@imperial.ac.uk
[d]Department of Materials, Imperial College London, London, SW7 2AZ, UK

† This publication is dedicated to Professor Martin Cowie, who forged a remarkable career exploring the reactivity of bimetallic complexes of bis(phosphine) ligands, including dppm. Rest in peace Uncle Marty.

hydrogen and carbon dioxide insertion reactions occurring during the catalytic cycle. There are two widely accepted mechanisms for heterogeneous Cu/ZnO catalysed CO_2 hydrogenation to methanol. Firstly, direct CO_2 hydrogenation, which proceeds *via* formate intermediates ($[O_2CH]^-$). Secondly, the reverse water–gas-shift reaction (RWGSR) and CO hydrogenation mechanism, in which CO_2 is converted to CO, followed by CO hydrogenation to methanol *via* formyl ($[OCH]^-$) and formaldehyde ($O{=}CH_2$) intermediates.[25] Formaldehyde is common to both mechanisms and is hydrogenated to a methoxy intermediate which is protonated to liberate methanol.[26]

It is hypothesized that most CO_2 hydrogenation occurs *via* the formate route,[37,38] with the Cu-sites responsible for the adsorption and dissociation of the H_2, while the ZnO inserts and activates the CO_2. The key steps in the formate mechanism are: (1) the reaction/absorption of CO_2 with ZnO possibly by insertion into surface hydride/hydroxide species to activate the carbon dioxide; (2) the reaction of the copper surface with hydrogen to form copper-hydrides or 'activated' hydrogen; and (3) the reaction between copper-hydride and the ZnO–carbon dioxide species, occurring at Cu–ZnO interfaces, to form formate intermediates.[39] Here, our objective is to isolate well-defined homogeneous metal complexes and clusters that react readily with hydrogen and carbon dioxide. We use these complexes as model compounds informing upon the structures and reactivity of metal hydride species.

There have been several prior investigations into the reactivity of well-defined homogeneous copper or zinc complexes with hydrogen or carbon dioxide.[30,40–45] Often, the copper or zinc hydride complexes were reacted with carbon dioxide to produce formate complexes.[30,40–48] For example, Bertrand and co-workers reported a transiently-formed copper(I) hydride complex [(^{Et}CAAC)CuH] (^{Et}CAAC = $(C_6H_3\text{-}2,6\text{-}^iPr_2)NC(Me_2)CH_2C(Et)_2C$; Fig. 1A) which reacted with CO_2 to yield a copper(I)-formate complex, [(^{Et}CAAC)Cu(O_2CH)].[27] Bertrand, Jazzar and co-workers also showed that a trinuclear $Cu^0_2Cu^I$ complex, [(^{Et}CAAC)Cu]$_3$, reduced CO_2 to CO, possibly paralleling the reactivity on copper surfaces during reductive CO_2 dissociation.[49] Gray, Sadighi and co-workers reported a hydride-bridged dicopper(I) cationic complex, [{(IDipp)Cu}$_2$(μ-H)][BF_4] (Fig. 1B), which reacted with CO_2 to provide a formate-bridged dicopper cation, [{(IDipp)Cu}$_2$(μ-O_2CH)][BF_4].[28] Tran, Bullock and co-workers isolated di-copper(I) dihydride bis(NHC) crystals and studied sequential carbon dioxide insertion reactions to give a di-copper(I)formate hydride crystal and, ultimately, a di-copper(I)bis(formate) speciation.[45] Whilst dimers were maintained in the crystal-to-crystal transformations, the equivalent complexes dissociated to monomers in solution. Appel and co-workers showed that a copper(I)-hydride complex, coordinated by a tris(phosphine) ligand, [{κ^3(*PPP*)-MeC(CH_2PPh_2)$_3$}CuH] (Fig. 1C), reacted with CO_2 to form a copper(I)-formate product, [{κ^3(*PPP*)-MeC(CH_2PPh_2)$_3$}Cu(O_2CH)].[29] Recently, Buss and co-workers reported a series of cationic tricopper(I) mono-, di- and trihydrido complexes, Cu_3H_x (x = 1–3) coordinated by tris(carbene) ligands, and showed that the CO_2 reactivity depended on the number of hydrido ligands (Fig. 1D).[30] The di- and trihydrido complexes, [LCu_3(μ-H)$_2$]BArF and [LCu_3(μ-H)$_3$] (L = C_6-1,3,5-{CH_2{NCN(Ar)CH_2CH_2}}$_3$-2,4,6-Et_3; Ar = C_6H_3-2,6-$^iPr_2$; BArF = B{C_6H_3-3,5-$(CF_3)_2$}$_4$), reacted with carbon dioxide to form copper formate products, whereas the monohydrido complex, [LCu_3(μ$_3$-H)][BArF]$_2$, was unreactive.

There is also precedent for reactions between zinc-hydride complexes and carbon dioxide.[32,33,50–54] For example, Parkin and co-workers reported a zinc(II)-hydride complex, coordinated by a tris(2-pyridylthio)methyl ligand, [{κ^3(*NNC*)-tptm}ZnH] (Fig. 1E), which reacted with CO_2 to afford a zinc(II)-formate complex, [{κ^3(*NNC*)-tptm}Zn(O_2CH)].[31] Okuda and co-workers reported CO_2 insertion into the Zn–H bond of [(Me_6tren)ZnH]BArF (Me_6tren = N{$(CH_2)_2NMe_2$}$_3$; Fig. 1F) to provide the zinc-formate product, [(Me_6tren)Zn(O_2CH)]BArF.[32] The zinc-hydride

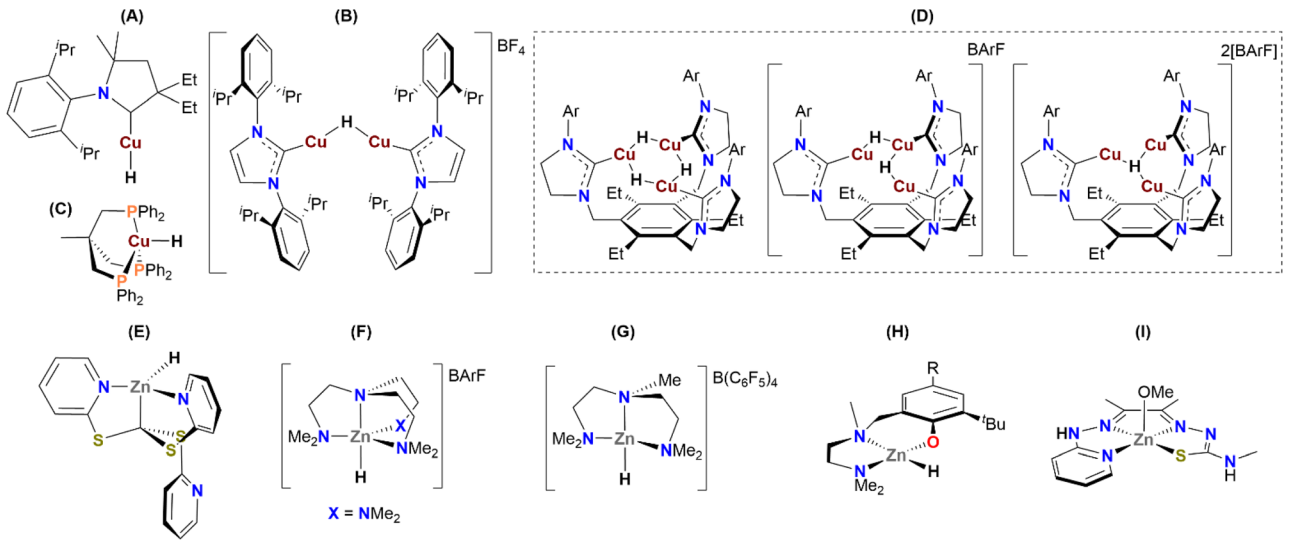

Fig. 1 Selected homogenous molecular copper and zinc complexes investigated for CO_2 hydrogenation in the literature.[27–36] Ar = C_6H_3-2,6-$^iPr_2$; BArF = B{C_6H_3-3,5-$(CF_3)_2$}$_4$; R = OMe, ^{t}Bu, NO_2.

complex of a related but less sterically hindered ligand, [(pmdta)ZnH][$B(C_6F_5)_4$] (pmdta = $MeN\{(CH_2)_2NMe_2\}_2$, Fig. 1G), produced a dimeric zinc-formate complex, [{(pmdta)$Zn(O_2CH)\}_2$][$B(C_6F_5)_4]_2$, when treated with CO_2.[33] Our group reported a series of zinc(II)-hydride complexes, coordinated by a κ^3(*NNO*)-di(amino)phenolate ligand, which reacted with CO_2 to provide zinc(II)-formate complexes (Fig. 1I).[34,35] It was shown that the rate of carbon dioxide insertion was equivalent or faster than the rate of carbon dioxide diffusion/solubilisation even at low pressures (in THF). Grapperhaus and co-workers reported an equilibrium between a zinc(II)–methanol complex, [(dmth)Zn(HOMe)] (dmth = diacetyl-2-(4-methyl-3-thiosemicarbazonate)-3-(2-pyridinehydrazonato)) and a zinc(II)-methoxide complex, [(**H**dmth)Zn(OMe)], facilitated by ligand protonation (Fig. 1H). The zinc(II)-methoxide complex reversibly inserts CO_2 into the Zn–OMe bond to form a zinc(II)-methylcarbonate complex, [(**H**dmth)Zn(O_2COMe)], which critically, facilitates CO_2 reduction; treatment chemically with $NaBH_4$, or electrochemically using a Pt electrode to generate Pt–H *via* the hydrogen evolution reaction (HER), produces methanol and generates a zinc(II)-formate complex, [(dmth)Zn(O_2CH)]. Ligand substitution of HCO_2^- for MeOH regenerates [(**H**dmth)Zn(OMe)], closing the CO_2 reduction cycle.[36]

The insertion of carbon dioxide into copper or zinc hydride bonds is quite well precedented but most of those hydride complexes were formed by metathesis reactions with alkali hydrides and silanes, or by the protonation of reactive metal alkoxides.[55,56] For example, copper hydride complexes were often prepared by reacting a copper precursor, *e.g.* $CuCl(PR_3)$ with $KHB(O^iPr)_3$, in the presence of strongly donating ligands (*i.e.* phosphines, carbenes, dithiophosphates or dithiocarbamates).[57] There is much less precedent for copper hydride formation by reaction of well-defined copper(I) complexes directly with hydrogen despite its importance in many of the catalytic cycles.[29,58–61] Further, the active site is often proposed to involve a copper–zinc interface, yet, there is very little precedent for well-defined heterometallic Cu/Zn complexes reacting with hydrogen or carbon dioxide.[62–64] Thus, we targeted well-defined copper and zinc complexes, including heterometallic complexes, and their reactivity with hydrogen and carbon dioxide. We selected a known copper(I) bis(phosphine) complex as the precursor since the chelating phosphine ligands may stabilise highly reactive intermediates and the ligand enables use of ^{31}P NMR spectroscopy to characterise products of insertion reactions.[65–67] In the heterogeneous catalysis, chemisorption of hydrogen is proposed to occur at Cu^0 active sites and may form Cu(I)–H surface species, akin to multimetallic oxidative addition, and play a key role in carbon dioxide reduction. Here, we targeted the reaction of the Cu(I) precursor with hydrogen to form copper(I) hydride complexes, but by H_2 heterolysis between a Brønsted basic phosphine ligand and the Cu(I) centre to which it is bound; we focus on multi-metallic complexes since surface active sites are proposed to involve several copper atoms/ions.[68,69] We also targeted heterometallic Cu(I)Zn(II) complexes to understand reactions with carbon dioxide, in particular whether CO_2 insertions would occur at zinc or copper sites.

Results

The synthesis and solid-state structure of the tri-copper(I) starting complex, [$Cu_3\{\mu{:}\kappa^3$(*PPC*)-dppm′$\}_2\{\mu{:}\kappa^2$(*PP*)-dppm′$\}$] (**1**; dppm′ = [$(Ph_2P)_2CH]^-$), was previously described and is formed by reacting mesitylcopper(I) ([CuMes]$_z$; z = 4, 5) with bis(diphenylphosphino) methane (dppm; $(Ph_2P)_2CH_2$) (Scheme 1).[65–67] The structure of complex **1** features three Cu^I centres coordinated by three anionic bis(phosphine) ligands, $[(Ph_2P)_2CH]^-$ (dppm′), in which the methylene carbon atom of dppm has been deprotonated. Complex **1** shows a solid-state structure with the following features: (1) two of the dppm′ ligands are κ^3(*PPC*)-coordinated to the Cu^I centres and the other dppm′ ligands is κ^2(*PP*)-coordinated, leaving a free anionic $CH_{methine}$; (2) two of the Cu centres are 4-coordinate and phosphine-coordinated, whereas one is 2-coordinate and only bound to anionic $CH_{methine}$ groups. We proposed that these structural features might allow **1** to react readily with hydrogen, carbon dioxide and/or organo-zinc reagents without involving any metal redox chemistry; as such, it affords an opportunity to investigate Cu(I) reactivity which might be relevant to catalyst surface reactivity.

First, the reaction of **1** with low pressures of H_2 (0.5 bar) was undertaken at 60 °C, in toluene, over 3 days. The reaction afforded [$Cu_5(\mu$-H)$(\mu_3$-H$)_2(\mu{:}\kappa^3$(*PPC*)-dppm′$)_2(\mu{:}\kappa^2$(*PP*)-dppm$)_2$] (**2**, Scheme 1) as a bright yellow solid, which was isolated in 63% yield. Complex **2** is a molecular cluster comprising 5 Cu^I centres, 2 anionic dppm′ ligands, 2 neutral dppm ligands and 3 hydride ligands. The reaction also affords neutral dppm ligand as a by-product; using *in situ* NMR spectroscopy to investigate the formation of **2** (from **1**) shows only the formation of **2** and free dppm (*i.e.* no intermediates). The $^{31}P\{^1H\}$ NMR spectrum for **2**, at 298 K in benzene-d_6, shows distinct resonances for each of the 8 phosphines with broadened singlets observed at 0.2, −0.6, −8.5 (2 PR_3), −13.9 and −14.6 ppm, and sharp doublets at −11.7 and −12.7 and ppm ($^2J_{P,P}$ = 27 Hz; Fig. S14). Variable temperature NMR spectroscopy did not show any changes (coalescence/splitting) to the broadened resonances from −80 to 70 °C. The peak broadening prevented use of 2-D NMR techniques (*e.g.* ^{1}H, ^{31}P-HMBC NMR spectroscopy) (Fig. S17 and S20).

The ^{1}H NMR spectrum of **2**, at 298 K in benzene-d_6, shows methine-C*H* resonances at 3.08 ppm, and two sets of methylene-CH_2 protons at 2.72 and 2.06 ppm, respectively. The methylene-CH_2 resonances were confirmed using ^{2}H-labelling experiments, *i.e.* after the reaction of **1** with D_2 and identification of D on the methylene unit in the ligand (Fig. S21). The copper-hydride resonances could not be located by ^{1}H or ^{2}H NMR spectroscopy, at room temperature or through variable temperature NMR experiments (−80 to 70 °C). This lack of a clear copper-hydride signal is proposed to arise from peak broadening due to the quadrupolar Cu (I = 3/2), combined with the likely fluxionality of the hydride ligands in solution (see SI). The FT-IR spectra of **2** and **2-d$_3$** are identical, indicating Cu–H stretches occur at very low frequencies (Fig. S23).

Crystals suitable for X-ray diffraction experiments were obtained by slow evaporation of a benzene solution of **2** at room

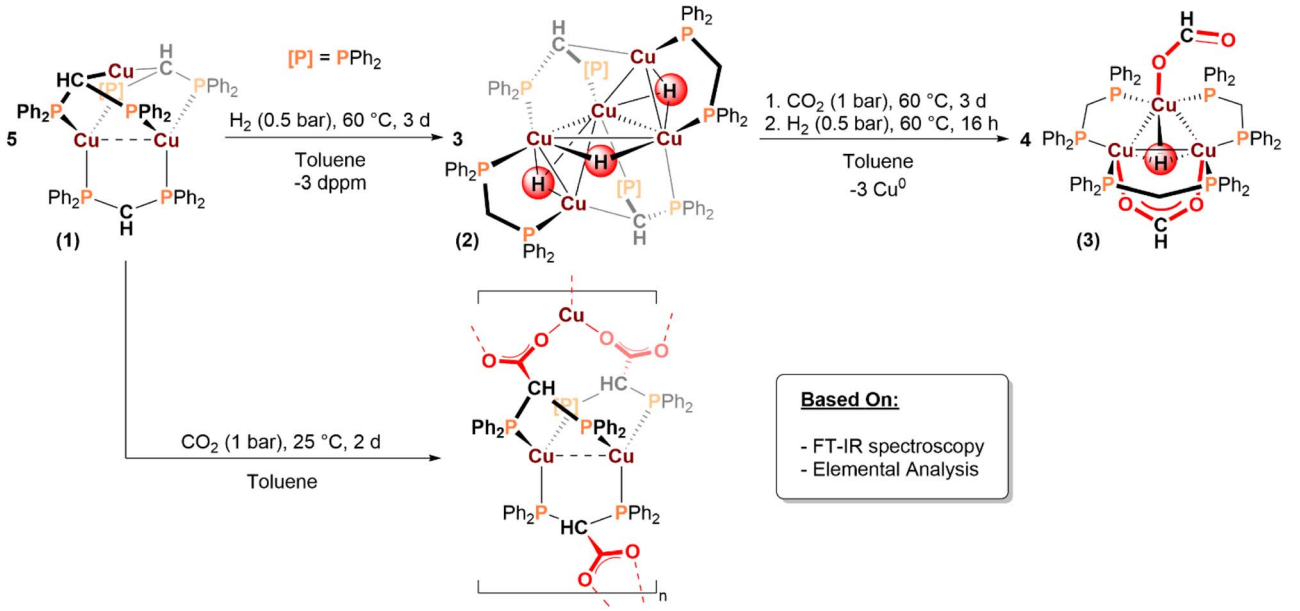

Scheme 1 Reactions of **1** with hydrogen to form $[Cu_5(\mu\text{-}H)(\mu_3\text{-}H)_2(\mu{:}\kappa^3(PPC)\text{-dppm}')_2(\mu{:}\kappa^2(PP)\text{-dppm})_2]$ (**2**) and, subsequently with carbon dioxide and hydrogen to form $[Cu_3(\mu_3\text{-}H)(\kappa^1(O)\text{-}O_2CH)(\mu{:}\kappa^2(OO)\text{-}O_2CH)(\mu{:}\kappa^2(PP)\text{-dppm})_3]$ (**3**).

temperature (Fig. 2). The solid-state structure shows 5 Cu^I centres and 3 hydrido ligands; the Cu centres form a distorted trigonal bipyramid, in which two apical Cu centres are located above and below an equatorial Cu_3-plane. The neutral dppm ligands are $\kappa^2(PP)$-coordinated to an apical and equatorial Cu(I) atom on the outer faces of the cluster, respectively. The anionic dppm′ ligands occupy the open faces of the cluster *via* $\kappa^3(PPC)$-coordination to the Cu(I) atoms (Fig. 2). The Cu–Cu bond lengths range from 2.683(1)–2.774(1) Å, which exceeds the sum of the covalent radii (2.24–2.64 Å)[70,71] but is significantly shorter than the sum of the van der Waals radii (3.84–4 Å),[72,73] The Cu–Cu bond length, in **2**, is also shorter than that observed for complex **1** (2.836(4) Å).[67] The intermetallic separation is, however, consistent with other neutral copper(I)-hydride cluster complexes (Table S3).[74–76] The orientation of the three Cu(I) centres in the equatorial sites is somewhat similar to bonding motifs observed at the Cu(111) surface; this surface is often invoked as a key interface during catalytic CO_2 hydrogenation.[77,78] Nonetheless, such analogies must be treated carefully since whilst the geometry may be somewhat similar, the Cu–Cu bond lengths in complex **2** are considerably longer than on a Cu(111) surface, where d_{Cu-Cu} is ~2.41 Å.[79] The Cu–P bond lengths range from 2.211(2)–2.318(2) Å, consistent with the average Cu–P bond length reported in **1** (2.317(5) Å).[67] Two of the hydrido ligands are μ_3-coordinated to an apical Cu(I) and two equatorial Cu(I) atoms, and one of the hydrido ligands is μ_2-coordinated between two equatorial Cu(I) centres. The Cu–H bond lengths range from 1.44(6)–1.94(6) Å, which are similar to bonds reported for other neutral Cu^I-hydride cluster complexes[74,75,80,81] and cationic bridging copper(I)-hydride complexes.[30,61] Given the inherent uncertainty in locating hydrido ligands by X-ray diffraction methods, the number and positions of the hydrido ligands in complex **2** were corroborated computationally by DFT. Three hydrido ligands were found to occupy nearly the exact locations as those determined by XRD, providing strong support for the experimental data (see Computational methods in the SI).

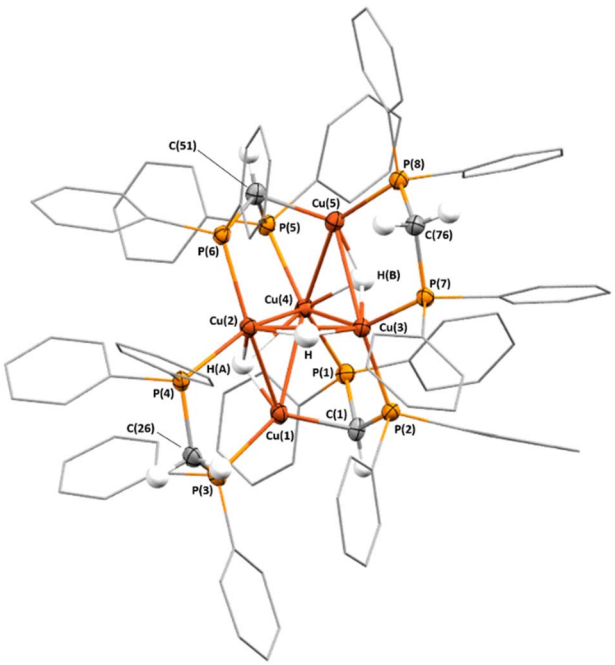

Fig. 2 Illustration of the solid-state structure of **2**·**4benzene** obtained from single crystal X-ray diffraction experiments. Displacement ellipsoids are drawn with 50% probability, and carbon atoms of the *P*-phenyl groups are drawn wireframe. For clarity, only one of two molecules in the asymmetric unit are depicted, and hydrogen atoms, aside for the bridging hydride ligands and methylene/methine protons, and lattice solvent are omitted.

As mentioned, there is precedent for copper(I) hydride complexes reacting with CO_2 to yield copper(I) formate

complexes.[27–30,45,49] To establish whether similar reactivity would be achieved using complex **2**, it was dissolved in toluene and exposed to 1 bar of carbon dioxide, at 60 °C, for 3 days which resulted in a colour change from bright yellow to colourless. The reaction product is [Cu_3(μ_3-H)(κ^1(*O*)-O_2CH)(μ:κ^2(*OO*)-O_2CH)(μ:κ^2(*PP*)-dppm)$_3$] (**3**; Scheme 1) but complete transformation of **2** into **3** did not occur until the solution was treated with H_2 (0.5 bar) and heated at 60 °C for 16 hours (Fig. S24–S26). Complex **3** features a Cu_3-core coordinated to two formate ligands. Labelling experiments, using D_2 and $^{13}CO_2$, confirmed that the formate ligands are produced by CO_2 insertion into the Cu–H bonds in **2** (the reactions to form **3-d$_3$** and **3-^{13}C** are described in the supplementary information). The tricopper complex is also coordinated to 3 neutral dppm ligands, which are κ^2(*PP*)-coordinated to the Cu(I) centres, indicating the complete protonation of the anionic dppm′ ligands in **2**. The ^{31}P{^{1}H} NMR spectrum shows a single resonance, at −8.4 ppm, indicating all phosphines are equivalent, in line with the solid-state structure (Fig. S27). The ^{1}H NMR spectrum of **3** contains a singlet, at 3.41 ppm, assigned to the methylene protons of the dppm ligands. It also contains a sharp singlet, at 9.55 ppm, assigned to the formate protons and a broadened singlet, at 1.57 ppm, assigned to the μ_3-hydrido ligand, the relative integrals for these resonances are 2 : 1, respectively (Fig. 3A and S28). When D_2 was used to afford **3-d$_3$**, the reaction product was characterised using ^{2}H NMR spectroscopy which revealed broadened resonances at 9.42, 3.29 and 1.52 ppm, which are assigned to the formate, methylene and μ_3-D groups, respectively (Fig. 3A and S29). The isotope experiments substantiate the assignment of the bridging hydrido ligand. Further, while the hydrido ligands in **2** were not observed using NMR spectroscopy (see above), the hydrido ligand resonance, in the ^{2}H NMR spectrum of **3-d$_3$**, may indicate that similar bonding occurs in **2-d$_3$** and that these bridging hydrides undergo CO_2 insertion to form the bridging formate ligands. The ^{1}H NMR spectrum of **3-^{13}C**, in which the carbon atom of the formate ligands has been ^{13}C-labelled, contains a doublet at 9.55 ppm ($^1J_{H,C}$ = 188 Hz), confirming its assignment as the formate proton (Fig. S30). Furthermore, the ^{13}C{^{1}H} NMR spectra of both **3** and **3-^{13}C** contain a singlet, at 168.3 ppm, confirming its assignment as the carbon atom of the formate ligands (Fig. S31 and S32). The FT-IR spectrum of **3** contains high intensity resonances at 1588, 1577 and 1569 cm^{-1}, assigned as the asymmetric ν(OCO) formate ligand stretches, and intense resonances at 1476 and 1426 cm^{-1}, assigned as the symmetric ν(OCO) formate stretching vibrations (Fig. S33). The combined spectroscopic features are consistent with data reported for some other copper(I) κ^1(*O*)- and κ^2(*OO*)-formate complexes.[27,40,42] In particular, a tri-copper(I) formate complex, [Cu_3(μ_3-H)(μ:κ^2(*OO*)-O_2CH)(dppm)$_3$][PF_6],[82] which was formed by reacting [Cu_8H_6(dppm)$_5$][PF_6] with CO_2. The previously reported copper(I) formate complex was cationic and contained a single formate ligand, bridging two Cu(I) centres. In contrast, complex **3** is neutral and features two bridging formate ligands (Table S4). The formate coordination chemistry is related to a previously reported tri-Cu(I) formate complex, [Cu_3(μ_3-H)(μ:κ^2(*OO*)-OAc)(κ^1(*O*)-OAc)(dppm)$_3$] (OAc = acetate), reported by Hayton and co-workers, which was formed by reacting copper(I) acetate with 0.5 equiv. of Ph_2SiH_2, and dppm ligand.[80] In both of these literature complexes, the Cu(I) clusters also feature a residual hydrido ligand and in both cases its stability was attributed to steric protection imparted by the Cu centres and dppm ligands.

Single crystals of **3·3benzene** suitable for X-ray diffraction experiments were obtained from a benzene solution of **3**, after hexane diffusion, at room temperature. The solid-state structure shows a trigonal planar Cu_3-core coordinated by 3 neutral dppm ligands and two formate ligands (Fig. 3B). One of the formate ligands adopts κ^2-bridging between 2 Cu centres *via* both its oxygen atoms, whereas the other is κ^1(*O*)-coordinated to only 1 Cu centre. The μ_3-hydrido ligand could not be located in the difference map, and crystals suitable for neutron diffraction could not be grown. As a result, DFT calculations were consulted to verify the position of the bridging hydrido ligand in **3**. The hydrido ligand was located in the centre and slightly off the plane of the Cu_3-ring and coordinated in a μ_3-fashion, in the same position as in the neutral acetate analogue, [Cu_3(μ_3-H)(μ:κ^2(*OO*)-OAc)(κ^1(*O*)-OAc)(dppm)$_3$] (OAc = acetate),[80] corroborating the assignment based on spectroscopic studies and ^{2}H-labelling (*vide supra*). In the absence of the location for the μ_3-hydrido ligand, each of the Cu centres are best described as basally distorted square pyramidal with the formate ligands occupying the apical site; the τ_5-parameters are 0.06, 0.20 and 0.21 for Cu(1), Cu(2) and Cu(3), respectively.[83,84] Once again, the orientation of the Cu_3 core is reminiscent of a Cu(111) monolayer, but with elongated Cu–Cu bond lengths.[79] The Cu(1)–Cu(2), Cu(1)–Cu(3) and Cu(2)–Cu(3) bond lengths in **3** are 2.9681(5), 2.9041(5) and 2.8071(5) Å, respectively. The Cu(2)–Cu(3) bond length is similar to the Cu–Cu bond lengths in **1** and **2**, however, the others are significantly longer.

The Cu(1)–O(1) bond length, to the κ^1-coordinated formate ligand, is 2.092(2) Å, and the Cu(2)–O(3) and Cu(3)–O(4) bond lengths, to the μ:κ^2-coordinated formate ligand, are 2.137(2) and 2.116(2) Å, respectively. The C–O bond lengths are all similar to one another (1.235(5)–1.253(3) Å), indicating charge delocalization across the formate ligands. Consistent with this charge delocalisation, the O–C–O bond angles are 128.3(3)° and 128.4(2)°. The structural parameters in **3** are consistent with reports of other copper formate complexes, *e.g.* [(κ^3(*PPP*)-triphos)Cu(κ^1(*O*)-O_2CH)][40] and [Cu_2(μ-O_2CH)(μ-*meso*-dpmppm)$_2$][BF_4] (see Table S4).[42] Compared to the cationic tri-copper complex, [Cu_3(μ_3-H)(μ:κ^2(*OO*)-O_2CH)(dppm)$_3$][PF_6] (Cu–O = 2.192(5) Å; C–O = 1.321(7); O–C–O = 105.2(5)°),[82] the Cu–O and C–O bond lengths are shorter, and the O–C–O bond angle is less acute. As noted above, the formation of **3** by treating **2** with CO_2 does not reach completion until the reaction is further charged with H_2. Further, in the reaction of **2** with only carbon dioxide, an additional species (to **3**) is observed by NMR spectroscopy which suggests there is at least one reaction intermediate which is consumed upon addition of excess H_2. The ^{1}H NMR spectrum of the crude product (prior to addition of hydrogen) shows signals for **3** and additional peaks for a second species. The intermediate shows a peak at 9.65 ppm, assigned to a formate ligand, and resonances at 4.86 (triplet; $^2J_{P,H}$ = 10 Hz), 2.98 and 2.47 ppm (2 × broad singlets), with relative integrals of ∼1 : 2 :

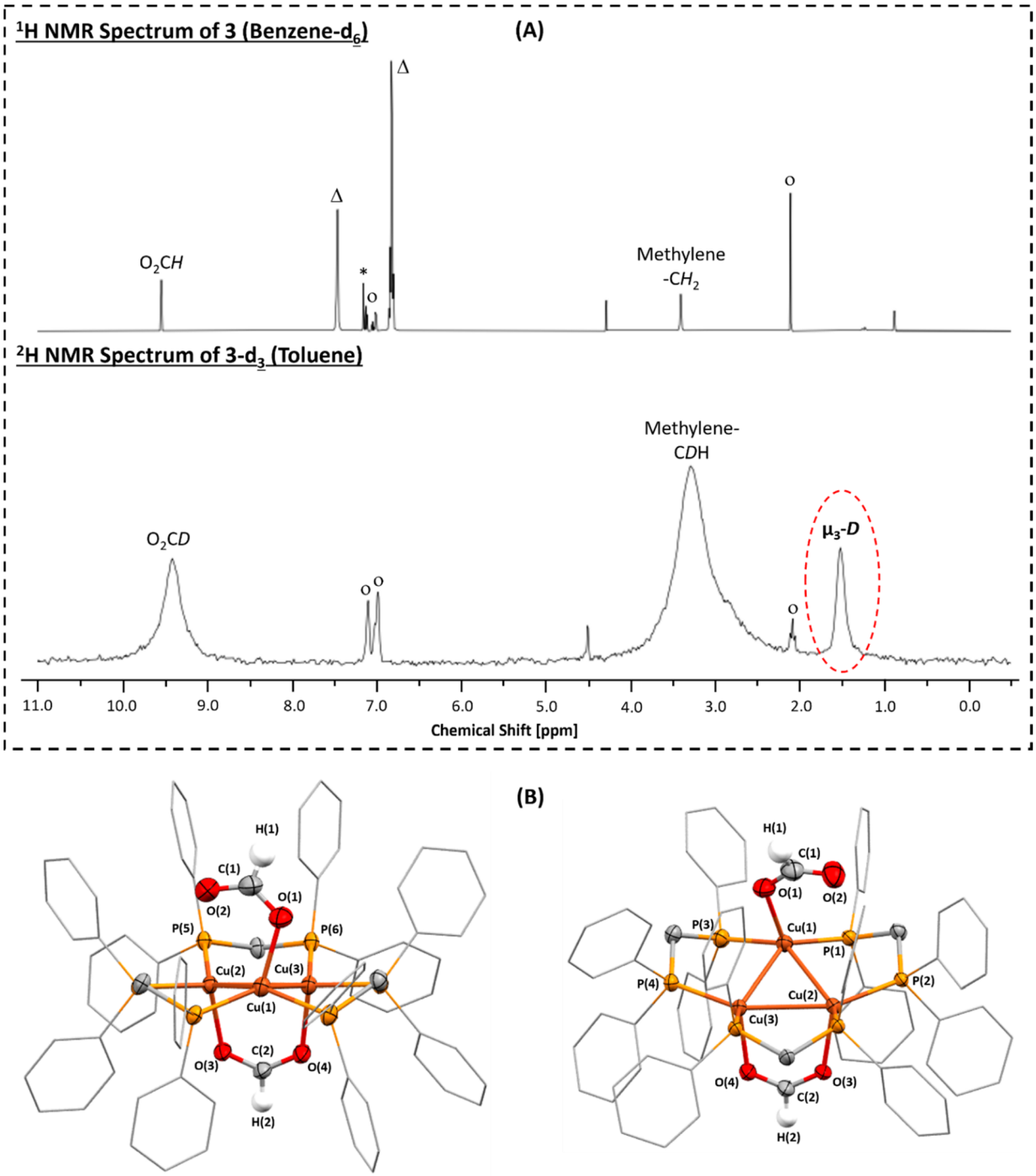

Fig. 3 (A) Stacked ^{1}H NMR (top; benzene-d$_6$, 298 K, 600 MHz) and ^{2}H NMR spectra (bottom; toluene, 298 K, 77 MHz) of **3** and **3-d$_3$**, respectively; the red highlighted resonance in the ^{2}H NMR spectrum of **3-d$_3$** is assigned as the μ$_3$-D resonance. Where other resonances marked * = benzene-d$_6$, Δ = PPh$_2$ and ○ = toluene. (B) Two orientations of the solid-state structure of **3·3benzene**. Displacement ellipsoids are drawn with 50% probability, and carbon atoms of the *P*-phenyl groups are drawn wireframe. For clarity, hydrogen atoms, except for H(1) and H(2), and lattice solvent are omitted. The μ$_3$-hydrido ligand could not be located in the difference map.

2, which are assigned to 1 anionic dppm′ and 2 neutral dppm ligand environments (see Fig. S24 and S25). On the basis of the NMR spectroscopic data, two potential structures are proposed: [Cu$_3$(μ$_3$-H)(O$_2$CH)(dppm′)(dppm)$_2$] (**2A**) or [Cu$_3$(O$_2$CH)$_2$(-dppm′)(dppm)$_2$] (**2B**; Scheme S1). The putative intermediate **2A** undergoes a single formate insertion and contains a bridging hydrido ligand, perhaps featuring the same trigonal planar Cu$_3$-core as **3**, with a dppm : dppm′ ratio of 2 : 1 (see Scheme S1 in SI for a discussion of possible reaction mechanisms). All attempts to selectively isolate the proposed intermediates for further

characterisation or to elucidate structures using ^{2}H- and ^{13}C-labelling experiments and NMR spectroscopy, were unsuccessful. Overall, when balancing the chemical reaction for the formation of **3**, 18 H-atoms should be required to cleanly form **3** from **2**, but only 9 hydrides are provided by **2**, consistent with the requirement for additional H_2 for the complete formation of **3**. To understand the reactivity of the formate ligands further, **3** was treated with a common organic reductant, pinacolborane (HBpin). No reaction occurred at room temperature, and upon gentle heating to 60 °C, **3** decomposes to Cu metal and unidentified organic by-products.

Next, the insertion reactions using carbon dioxide were investigated; complex **1** was reacted with CO_2 to understand whether there would be any insertion into its Cu–C bonds, as anticipated from the prominence of organocopper chemistry in carboxylation reactions.[85,86] Exposure of **1** to CO_2 (1 bar), in toluene at room temperature, resulted in a colour change from yellow to nearly colourless with concomitant precipitation of a white solid. Attempts to solubilize the reaction product in benzene-d_6, CD_2Cl_2, THF-d_8 and acetone-d_6 were unsuccessful, suggesting the formation of a copper-carboxylate polymer/aggregate. The solid was analysed by FT-IR spectroscopy which showed high intensity absorptions at 1425 and 1307 cm^{-1}, assigned to asymmetric and symmetric carboxylate stretches and consistent with bridging carboxylate ligands. The solid's elemental analysis was consistent with the molecular formula $C_{75}H_{63}Cu_3P_6 \cdot 3CO_2$, *i.e.* reaction of 1 equiv. CO_2 per dppm′ in **1** (see Fig. S34, SI). Therefore, the product is proposed to be a polymeric copper carboxylate species, formed by CO_2 insertion into Cu–C bonds and by reaction (at C) with the methine carbon atom of the κ^2(*PP*)-coordinated dppm′ ligand (Scheme 1).

Another objective is to understand the reactivity of well-defined heterometallic Cu(I) and Zn(II) complexes, since Cu/Zn(II) interfaces are critical as active sites in heterogeneous carbon dioxide hydrogenation catalysis. Thus, the reaction of tri-copper(I) complex **1** with organo-Zn^{II} complexes was used to try to isolate mixed metal complexes. The organo-zinc reagent was $[Zn(C_6F_5)_2]$ since we reasoned its relatively high Lewis acidity should enable reaction with the anionic $CH_{methine}$ group, or even insertion into the Cu–$CH_{methine}$ bonds. Treating **1** with $[Zn(C_6F_5)_2]$, in toluene, produced an immediate colour change from yellow to colourless, affording $[Cu_2(\mu{:}\kappa^3(PPC)\text{-dppm}')_2\{Zn(C_6F_5)_2\}_2]$ (**4**, Scheme 2). Single crystals suitable for X-ray diffraction experiments were obtained by slow evaporation of a benzene solution of the product. The solid-state structure shows that **4** is a tetrametallic Cu_2Zn_2-complex with the $Zn(C_6F_5)_2$ coordinated to the anionic –$CH_{methine}$ groups of the dppm′ ligands. There is also κ^2(*PP*)-coordination of two dppm′ ligands to two Cu^{I} centres in the core of the structure (Fig. 4). Two different isomers were identified: a *cis*-isomer where the two zinc centres are on the same side (both above/below) of the central Cu_2-plane (***cis*-4**; Fig. 4A), and a *trans*-isomer, in which the zinc atoms are located above and below the central di-Cu(I) plane (***trans*-4**; Fig. 4B). The Cu(I) centres in both ***cis*-4** and ***trans*-4** both exhibit T-shaped coordination geometry, with P–Cu–P and P–Cu–Cu bond angles of 168.04(2)° and 90.94(1)–96.42(1)° in ***cis*-4**, and 171.20(1)° and 88.57(1)–96.05(1)° in ***trans*-4**, respectively. There are short Cu···F (from *ortho*-C_6F_5) distances of 2.869 and 2.719 Å in ***cis*-4** and ***trans*-4**, respectively. These distances lie well within the sum of the van der Waals radii (3.27 Å) and imply there is some cationic charge on each copper(I) atom.[72] The Zn centres in each isomer exhibit trigonal planar geometry, with the Σ(CZnC) angles equal to 359.8(2)° in both isomers (theoretical = 360°), implying anionic charge on zinc. Overall, the complex is polarised as a cuprous zincate. The Cu–Cu bond length in ***cis*-4** is 2.6736(4) Å, which is significantly shorter than the Cu–Cu bond lengths in **1** (2.836(4) Å)[67] and **3** (2.8071(5)–2.9681(5) Å). The Cu–Cu bond lengths are close to those found in **2** (2.682(1)–2.772(1) Å) and in several literature copper(I) cationic clusters, *e.g.* $[Cu_2(\mu\text{-dcpm})_2][BF_4]_2$ (dcpm = $(Cy_2P)_2CH_2$; Cy = cyclohexyl; Cu–Cu = 2.691(2) Å)[87] and $[Cu_3(\mu_3\text{-H})(\mu\text{-dppy})_4][ClO_4]_2$ (dppy = py-2-PPh_2; py = pyridyl; Cu–Cu = 2.701(1), 2.749(1), 2.723(1) Å).[88] The Cu–Cu bond length in ***trans*-4** is 2.8235(4) Å, and may indicate slightly reduced polarisation between the cationic Cu and anionic Zn centres. While the Cu–Cu distances in both ***cis*-4** and ***trans*-4** are longer than the sum of the covalent radii (2.24–2.64 Å),[70,71] they are significantly shorter than the sum of the van der Waals radii (3.84–4 Å).[72,73] The Cu–P bond lengths in **4** (2.2182(3)–2.2283(3) Å) are significantly shorter than those found in **1** (average = 2.317(5) Å),[67] and **3** (2.2497(7)–2.2910(7) Å). They are, once again, similar to those found in **2** (2.209(2)–2.318(1) Å) and in some literature cationic copper(I) phosphine complexes $[Cu(P^tBu_3)_2][PF_6]$ (Cu–P = 2.2187(6) Å)[89] and $[(Me_3P)_2Pd(\mu\text{-2-}C_6F_4PPh_2)_2Cu][PF_6]$ (Cu–P = 2.217(2), 2.214(2) Å).[90] The Zn–C bond lengths range from 2.008(1)–2.082(1) Å in ***cis*-4**, and 2.005(1)–2.097(1) Å in ***trans*-4**, which are longer than in neutral Zn-aryl complexes[91] but consistent with prior reports of complexes featuring anionic organo-zincates (see Table S5).[92] Despite the different orientations of the –$Zn(C_6F_5)_2$ moieties in the isomers, the Zn···Zn distances are similar, at 7.304 and 8.365 Å in ***cis*-4** and ***trans*-4**, respectively.

The $^{31}P\{^{1}H\}$ NMR spectrum of **4** contains two singlets, at 15.6 and 15.2 ppm (CD_2Cl_2), in an approximate 5 : 2 ratio, respectively. These are tentatively assigned to differing quantities of the *cis*- and *trans*-isomers of **4**. These signals are shifted from those observed for **1** which are at 0.8 and −18.8 ppm (benzene-d_6; Fig. S10 and S35). The higher chemical shifts for **4** are consistent with the incorporation of Lewis acidic zinc into the complex. The ^{19}F NMR spectrum contains two sets of *ortho*-, *meta*- and *para*-F resonances, also in an ∼5 : 2 ratio. One set of resonances is located at −116.8, −158.8, and −162.6 ppm, and the second set is located at −117.3, −159.2, and −163.2 ppm; both sets of resonances are shifted relative to $[Zn(C_6F_5)_2]$ (Fig. S36 and S37). The ^{1}H NMR spectrum of **4** contains resonances at 3.83 and 3.76 ppm which are assigned to the –$CH_{methine}$ protons, also integrating in a 5 : 2 ratio, respectively (Fig. S38). All attempts to separate the *cis*- or *trans*-isomers proved unsuccessful, immediately forming the same 5 : 2 ratio of isomers perhaps suggesting a dynamic equilibration between them. Treating complex **1** with $[Zn(Mes)_2]$, a reagent which should be less Lewis acidic than $[Zn(C_6F_5)_2]$, failed to result in any reaction and both starting species remained unreacted in

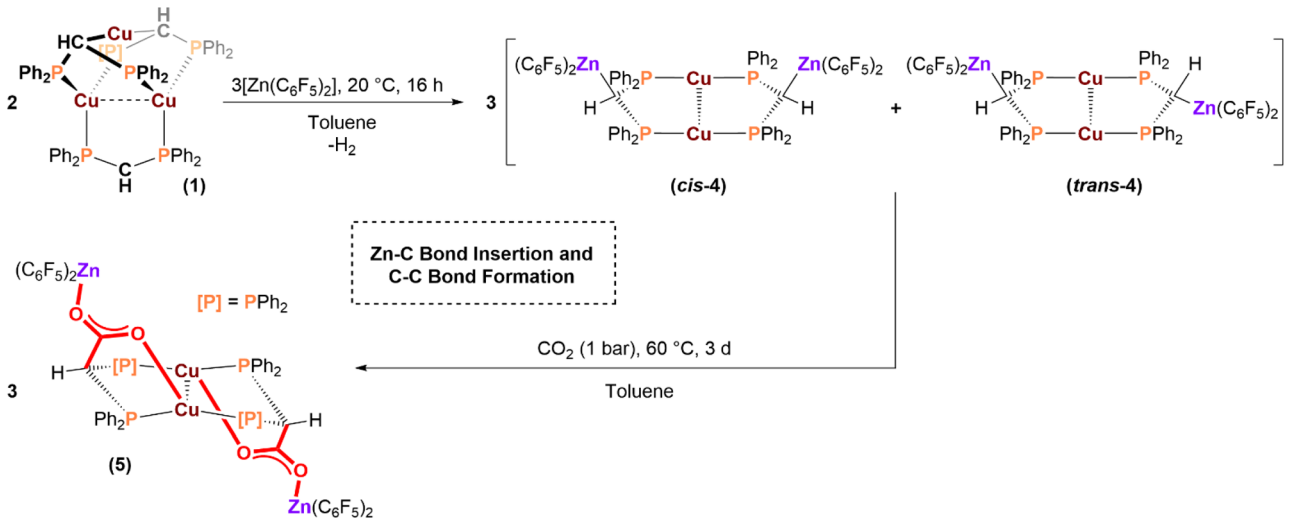

Scheme 2 The reaction of **1** with $Zn(C_6F_5)_2$ to form heterometallic di-copper(I)–di-Zn(II) complex **4** as *cis*- and *trans*-isomers of $[Cu_2(\mu{:}\kappa^3(PPC)\text{-dppm}')_2\{Zn(C_6F_5)_2\}_2]$ (***cis*-4** and ***trans*-4**). The subsequent reaction of **4** with CO_2 affords heterometallic complex $[Cu_2(\mu{:}\kappa^4(PPOO)\text{-dppm}'')_2\{Zn(C_6F_5)_2\}_2]$ (**5**).

solution even over pro-longed periods. Therefore, it seems that the higher Zn(II) Lewis acidity of $[Zn(C_6F_5)_2]$ is relevant to its successful coordination by the anionic methine group of dppm′, either by coordination to a free $[CH(PPh_2)_2]^-$ or *via* insertion into a Cu–$CH_{methine}$ bond.

Next, the reactivity of **4** with CO_2 and H_2 was investigated. Treating **4** with CO_2, at 1 bar in toluene solution and at room temperature, did not result in any reaction. When the solution was heated to 60 °C, there was complete (quantitative) conversion into $[Cu_2(\mu{:}\kappa^4(PPOO)\text{-dppm}'')_2\{Zn(C_6F_5)_2\}_2]$ (**5**; Scheme 2) which was isolated in 72% yield. Complex **5** is the product of CO_2 insertion into the Zn–$C_{methine}$ bond and results from a new C–C bond forming between the carbon atom of CO_2 and the methine carbon of the ligand. The reaction can be viewed as producing carboxylated dppm′, henceforth referred to as dppm″. The dppm″ ligand is $\kappa^2(PP)$-coordinated to the two Cu(I) centres, and its carboxylate moiety bridges, *via* the O-donors, between the Zn(II) and Cu(I) centres (Scheme 2). The $^{31}P\{^1H\}$ NMR spectrum of **5** shows a singlet, at 11.2 ppm, shifted ~4 ppm to lower frequency relative to **4** and indicative of reduced cationic charge on the Cu(I) centres (Fig. S41). The ^1H NMR spectrum shows a peak at 5.09 ppm assigned to the $HC_{methine}$ group (Fig. S42); this resonance is shifted by ~1.3 ppm to higher frequency relative to **4**. The ^{19}F NMR spectrum shows resonances at −117.3, −158.1 and −163.0 ppm, assigned to the *o*-, *p*- and *m*-(C_6F_5) nuclei, respectively (Fig. S44). The FT-IR spectrum of **5** contains absorptions at 1573 and 1445 cm^{-1}, assigned as the asymmetric and symmetric carboxylate stretches, respectively (Fig. S45).

The $^{13}C\{^1H\}$ NMR spectrum contains a singlet at 178.6 ppm, assigned to the $[RCO_2]^-$ carbon atom and with a chemical shift consistent for a carboxylate group (Fig. S46). Single crystals of

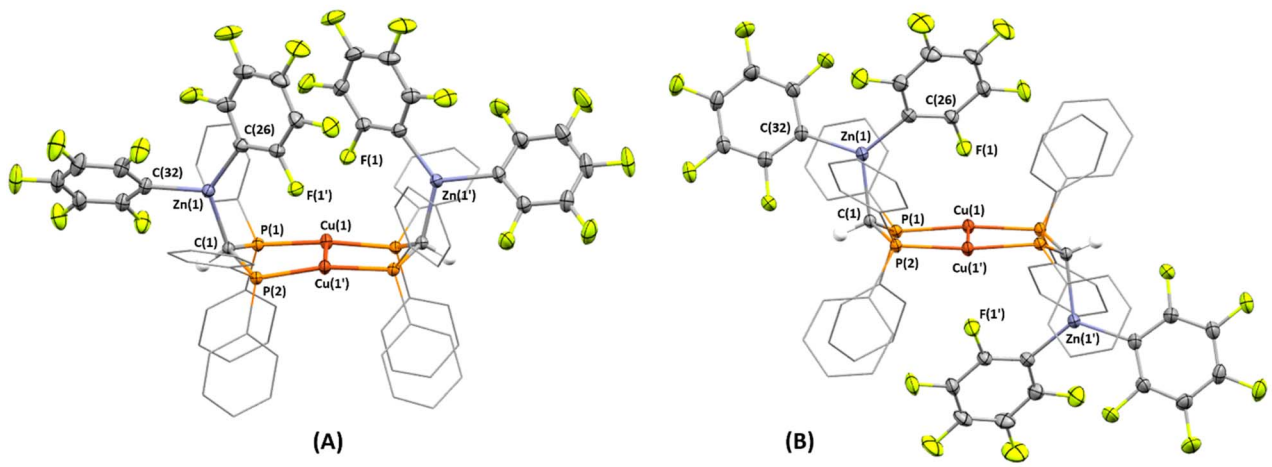

Fig. 4 Solid-state structures of (A) **cis-4·2benzene** and (B) ***trans*-4·3benzene**. Displacement ellipsoids are drawn with 50% probability, and carbon atoms of the *P*-phenyl groups are drawn wireframe. For clarity, hydrogen atoms and lattice solvent are omitted.

5·2benzene suitable for X-ray diffraction experiments were obtained by slow evaporation of a benzene solution of **5** at room temperature (Fig. 5). The –[Zn(C_6F_5)$_2$] groups are coordinated in a *trans*-arrangement, with a Zn···Zn distance of 10.852 Å. The coordination geometry of the Cu centres is best described as distorted trigonal pyramidal, with the phosphine- and carboxylate-donors residing in a trigonal-plane, and the Cu–Cu bond occupying the apical coordination site. The Cu–Cu bond length (2.6792(4) Å) is consistent with that found in ***cis*-4** and significantly shorter than that found in ***trans*-4**. While the Cu(1′)–P(2) bond length (2.1977(3) Å) is consistent with those found in **4**, the Cu(1)–P(1) bond length (2.2779(3) Å) is significantly longer. The C–O bond lengths are relatively similar to one another, with C(2)–O(1) and C(2)–O(2) being 1.267(2) and 1.250(2) Å, respectively, and are consistent with charge delocalisation across the carboxylate ligand. The coordination geometry of the Zn(II) centres is best described as T-shaped, with C(27)–Zn(1)–C(33), C(27)–Zn(1)–O(2) and C(33)–Zn(1)–O(2) bond angles equal to 148.58(6)°, 104.98(5)° and 105.36(5)°, respectively. Given that the coordination geometry of Zn(II) is no longer trigonal planar, as is the case in **4**, charge delocalisation seems to favour charge polarisation towards Cu(I) rather than Zn(II) in the precursor complex. Moreover, the Zn–C bond lengths in **5** are 1.970(1) and 1.970(2) Å, which are significantly shorter than in **4** and consistent with the evolution into neutral Zn(aryl)$_2$ complexes. However, while the Cu–O bond length in **5** (2.0772(9) Å) is consistent with literature copper(I) complexes featuring an anionic O-donor coordinated to Cu (see Table S6),[80,93] the Zn–O bond length (2.020(1) Å) is also similar to that reported for complexes featuring an anionic O-donor coordinated to Zn^{II}, indicative of charge delocalisation within the carboxylate group (see Table S6).[94–96]

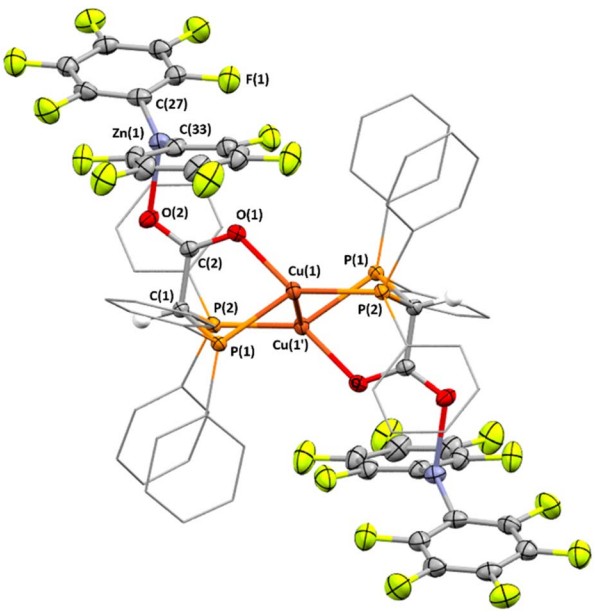

Fig. 5 Solid-state structure of **5·2benzene**. Displacement ellipsoids are drawn with 50% probability, and carbon atoms of the *P*-phenyl groups are drawn wireframe. For clarity, hydrogen atoms, except for the methine protons, and lattice solvent are omitted.

In an attempt to isolate a copper/zinc-hydride complex, **4** was treated with H_2 (1 bar) in benzene-d_6. There was no reaction at room temperature but upon gentle heating, 60–80 °C, the complex decomposed, depositing some Cu metal onto the Schlenk flask walls and evolving C_6HF, as identified by ^{19}F NMR spectroscopy. Finally, complex **5** was treated with H_2 and, in separate reactions, with various metal hydrides, including CaH_2 or HBpin, to determine whether further hydrogenation of the carboxylate ligand was feasible. In all cases, no reaction occurred at room temperature, and heating benzene-d_6 solutions to 60–80 °C resulted in decomposition, with the only assigned product, by ^{19}F NMR spectroscopy, being C_6HF_5.

Discussion

The tri-copper(I) precursor complex **1** was successfully used to identify and characterise small-molecule clusters formed by reactions with hydrogen, carbon dioxide and Lewis acidic Zn(II) species. Complex **2** is a copper(I)-hydride cluster formed by heterolysis of dihydrogen at the copper(I) sites and the Brønsted basic carbanion backbone of the chelating phosphine ligands. It reacts with carbon dioxide, *via* a process which is assisted by additional hydrogen, to form a copper(I)-formate complex, **3**. Complex **4** is the product of the Cu(I) precursor reaction with zinc(II) precursors to form a heterometallic Cu_2Zn_2-bis(phosphine) complex. It reacts at low pressures (1 bar) of CO_2 to form a heterometallic Cu_2Zn_2 complex featuring bridging carboxylate ligands. In all these reactions, the copper(I) sites readily form Cu-hydrides even when the starting material is exposed to relatively low pressures (concentrations) of hydrogen gas. In contrast, for the heterometallic complexes there was no equivalent Zn–H formation. The copper(I)-hydrides insert carbon dioxide readily to form Cu(I) formate complexes, even using low pressures of carbon dioxide. The heterometallic Cu(I)/Zn(II) complexes react with carbon dioxide to form carboxylates that bridge between the two metals and may facilitate charge delocalisation between them. The complexes suggest that cuprous zincate structures may help to increase reactivity at Zn(II) sites. It is interesting that these alkyl-zincates react with the electrophilic carbon, of carbon dioxide, to form new C–C bonds and carboxylate bridging ligands. There are few examples of low pressure carbon dioxide insertion into alkyl–zinc bonds to effect carboxylation;[97,98] Hou has reported the alkylative carboxylation of allenamides or ynamides using carbon dioxide, dialkyl zinc reagents and a Cu(I) catalyst.[99,100] The carboxylation reactivity using complex **4**, which combines Cu(I) and Zn(II) sites, should be investigated for other carboxylations, both stoichiometric and catalytic, using carbon dioxide.[101] One challenge that must be overcome in any catalytic chemistry targeting alcohols is the need to further reduce the metal formate and carboxylate species – in this work, preliminary attempts to achieve these reductions have proved unsuccessful. In future, the reactions of cuprous formate (*e.g.* complexes **3**) or copper(I) zinc(II) formates (*e.g.* complex **5**) with higher pressures of hydrogen gas should be undertaken. Recent work has established that cuprous hydride complexes can reduce aldehydes (to alkoxides) and esters.[102] Further reactions should be

explored between the cuprous (zinc) formate complexes and stable cuprous hydride complexes, *e.g.* Strykers copper hydride reagent or even, perhaps, complex **2**.[103,104]

The objective was to investigate the reactivity of well-defined organo-copper(I) and Zn(II) complexes as possible mimics for the active site surfaces of heterogeneous catalysts. The chemistry observed in this work may be relevant, but caution must be applied since heterogeneous catalytic intermediates likely involve multiple metals and are mobile across the catalyst surface. Nonetheless, the reactions of the well-defined complexes, in this work, indicate that hydrogen can be activated heterolytically at Cu(I) sites in the presence of a suitable ligand environment (*i.e.* strongly Brønsted basic ligands), and is not limited to Cu(0) sites *via* oxidative addition, akin to H_2 chemisorption on a heterogenous surface. The other key reagent, carbon dioxide, reacts readily with both cuprous hydrides and organozinc reagents, and forms metal carboxylate ligands that often adopt bridging coordination modes to the metals. These chemistries are consistent with the proposed speciation occurring during the first steps of the formate carbon dioxide hydrogenation mechanism.[26] In heterogeneous catalysis, Cu(I) surface species are certainly feasible, particularly during hydrogen activation,[105] and hence the current work may inform upon speciation during hydrogen activation at Cu, either by chemisorption or heterolysis. Although, ZnO surfaces are not usually considered as negatively charged, in heterogeneous catalysis, this work highlights that cuprous zincate interfaces can introduce charge polarisation from Cu(I) to Zn(II); this zincate-induced polarisation may modulate the catalytic activity, for example, enabling carbon dioxide activation *via* reaction at its electrophilic carbon atom and providing a future route to C–C bond formation during the reductions. The formation of higher alkanol/alkene products would be very valuable and is generally not achieved using only Cu/ZnO catalysts. Future work should continue to prioritise heterometallic clusters featuring hydrides and formates as ligands. Following the success of the complexes described in this work, understanding the onward speciation during later stages of the reduction or coupling chemistry is a future target. The complexes described in this work may also enable reactions with s-block metals, like K, Mg, and Ca, which are well known to form metal zincates;[64,106–108] for example, heteromagnesium complexes showed unusual reactivity with formyl groups and are common promoters of Cu/ZnO heterogeneous catalysts.[109–114]

Conclusions

A trimetallic copper(I) complex, $[Cu_3\{\mu{:}\kappa^3(PPC)\text{-dppm}'\}_2\{\mu{:}\kappa^2(PP)\text{-dppm}'\}]$ (**1**; dppm′ = $[(Ph_2P)_2CH]^-$) was used to investigate reactions with hydrogen, carbon dioxide and Lewis acidic organo-zinc precursors. Well-defined copper(I) hydride and formate clusters and a heterometallic Cu(I)Zn(II) carboxylate complex were isolated and characterised. The tri-Cu(I) complex **1** reacted with hydrogen to form a penta-copper-hydride cluster complex, $[Cu_5(\mu\text{-H})(\mu_3\text{-H})_2(\mu{:}\kappa^3(PPC)\text{-dppm}')_2(\mu{:}\kappa^2(PP)\text{-dppm})_2]$ (**2**). Complex **2** reacted with carbon dioxide to form a tri-copper(I)-hydrido-bis(formate) complex, $[Cu_3(\mu_3\text{-H})(\kappa^1(O)\text{-O}_2\text{CH})(\mu{:}\kappa^2(OO)\text{-O}_2\text{CH})(\mu{:}\kappa^2(PP)\text{-dppm})_3]$ (**3**). A mixed metal copper(I)zinc(II) complex, $[Cu_2(\mu{:}\kappa^3(PPC)\text{-dppm}')_2\{Zn(C_6F_5)_2\}_2]$ (**4**), was formed by treating **1** with $[Zn(C_6F_5)_2]$ and features cationic Cu(I) sites and anionic zincate(II) moieties. It reacted with carbon dioxide to form a new cluster Cu^IZn^{II}-carboxylate complex, $[Cu_2(\mu{:}\kappa^4(PPOO)\text{-dppm}'')_2\{Zn(C_6F_5)_2\}_2]$ (**5**), in which CO_2 inserts into a Zn–C bond to form a new C–C bond and bridging carboxylate species. While neither **3** or **5** reacted with sources of hydride, such as HBpin or CaH_2, to reduce CO_2, future work will investigate other hydride sources, such as silanes, for carbon dioxide hydroelementation.

Overall, the Cu(I) complex reacted with hydrogen to form a molecular hydride species which reduced CO_2 to form a formate complex. In contrast, the heterometallic Cu(I)Zn(II) complex reacted with carbon dioxide to form a metal carboxylate species. In the future, other heterometallic Cu(0/I)Zn(II) complexes should be used to explore the generality of the reactivity. The cuprous zincates may help to moderate intermetallic polarisation and electron transfer processes. These results may even, in the longer term, help inform upon roles for copper and zinc species in CO_2 hydrogenation catalysts. It remains a long-standing goal to discover homogeneous carbon dioxide hydrogenation catalysts able to form higher (C_2 and above) alcohols and alkenes, particularly using earth abundant metals like Cu and Zn.

Author contributions

BEC: conceptualization, data curation, formal analysis, investigation, methodology, validation, visualization, writing – original draft. AP: conceptualization, writing – review & editing. MSPS: conceptualization, funding acquisition, project administration, supervision, writing – review & editing. CKW: conceptualization, funding acquisition, project administration, resources, supervision, writing – review & editing.

Conflicts of interest

There are no conflicts to declare.

Data availability

CCDC 2269234–2269239 (**1–6**) contain the supplementary crystallographic data for this paper.[115a–f]

The data supporting this article have been included as part of the supplementary information (SI). Supplementary information: full experimental details and procedures, tables of structural and spectroscopic metrics for comparison with similar compounds reported in the literature, characterisation data (^1H, ^2H, $^{13}C\{^1H\}$, $^{31}P\{^1H\}$ and $^{19}F\{^1H\}$ NMR, FT-IR, and crystallographic details), and computational methods. See DOI: https://doi.org/10.1039/d5sc05666g.

Acknowledgements

This work was supported by the UK Engineering and Physical Sciences Research Council (EPSRC) (grant number EP/S018603/1) and the UK Catalysis Hub (EP/R026645/1).

Notes and references

1 M. Bowker, Methanol Synthesis from CO_2 Hydrogenation, *ChemCatChem*, 2019, **11**, 4238–4246.

2 S. Enthaler, J. von Langermann and T. Schmidt, Carbon Dioxide and Formic Acid - The Couple for Environmental-Friendly Hydrogen Storage?, *Energy Environ. Sci.*, 2010, **3**, 1207–1217.

3 G. A. Olah, Towards Oil Independence Through Renewable Methanol Chemistry, *Angew. Chem., Int. Ed.*, 2013, **52**, 104–107.

4 G. A. Olah, G. K. Surya Prakash and A. Goeppert, Anthropogenic Chemical Carbon Cycle for a Sustainable Future, *J. Am. Chem. Soc.*, 2011, **133**, 12881–12898.

5 P. Borisut and A. Nuchitprasittichai, Methanol Production via CO_2 Hydrogenation: Sensitivity Analysis and Simulation-Based Optimization, *Front. Energy Res.*, 2019, **7**, 81.

6 D. S. Marlin, E. Sarron and Ó. Sigurbjörnsson, Process Advantages of Direct CO_2 to Methanol Synthesis, *Front. Chem.*, 2018, **6**, 446.

7 S. Navarro-Jaén, M. Virginie, J. Bonin, M. Robert, R. Wojcieszak and A. Y. Khodakov, Highlights and Challenges in the Selective Reduction of Carbon Dioxide to Methanol, *Nat. Rev. Chem.*, 2021, **5**, 564–579.

8 L. C. Grabow and M. Mavrikakis, Mechanism of Methanol Synthesis on Cu Through CO_2 and CO Hydrogenation, *ACS Catal.*, 2011, **1**, 365–384.

9 G. C. Chinchen, P. J. Denny, D. G. Parker, M. S. Spencer and D. A. Whan, Mechanism of Methanol Synthesis from CO_2/CO/H_2 Mixtures over Copper/Zinc Oxide/Alumina Catalysts: Use of ^{14}C-Labelled Reactants, *Appl. Catal.*, 1987, **30**, 333–338.

10 J. Nakamura, I. Nakamura, T. Uchijima, T. Watanabe and T. Fujitani, Model Studies of Methanol Synthesis on Copper Catalysts, *Stud. Surf. Sci. Catal.*, 1996, **101**, 1389–1399.

11 M. Bukhtiyarova, T. Lunkenbein, K. Kähler and R. Schlögl, Methanol Synthesis from Industrial CO_2 Sources: A Contribution to Chemical Energy Conversion, *Catal. Lett.*, 2017, **147**, 416–427.

12 S. Kattel, P. J. Ramírez, J. G. Chen, J. A. Rodriguez and P. Liu, Active Sites for CO_2 Hydrogenation to Methanol on Cu/ZnO Catalysts, *Science*, 2017, **355**, 1296–1299.

13 J. Nakamura, I. Nakamura, T. Uchijima, Y. Kanai, T. Watanabe, M. Saito and T. Fujitani, A Surface Science Investigation of Methanol Synthesis over a Zn-Deposited Polycrystalline Cu Surface, *J. Catal.*, 1996, **160**, 65–75.

14 J. Nakamura, Y. Choi and T. Fujitani, On the Issue of the Active Site and the Role of ZnO in Cu/ZnO Methanol Synthesis Catalyts, *Top. Catal.*, 2003, **22**, 277–285.

15 M. Behrens, F. Studt, I. Kasatkin, S. Kühl, M. Hävecker, F. Abild-Pedersen, S. Zander, F. Girgsdies, P. Kurr, B.-L. Kniep, M. Tovar, R. W. Fischer, J. K. Nørskov and R. Schlögl, The Active Site of Methanol Synthesis over Cu/ZnO/Al_2O_3 Industrial Catalysts, *Science*, 2012, **336**, 893–897.

16 S. Kuld, C. Conradsen, P. G. Moses, I. Chorkendorff and J. Sehested, Quantification of Zinc Atoms in a Surface Alloy on Copper in an Indistrial-Type Methanol Synthesis Catalyst, *Angew. Chem., Int. Ed.*, 2014, **53**, 5941–5945.

17 S. Kuld, M. Thorhauge, H. Falsig, C. F. Elkjær, S. Helveg, I. Chorkendorff and J. Sehested, Quantifying the Promotion of Cu Catalysts by ZnO for Methanol Synthesis, *Science*, 2016, **352**, 969–974.

18 T. Fujitani, I. Nakamura, T. Uchijima and J. Nakamura, The Kinetics and Mechanism of Methanol Synthesis by Hydrogenation of CO_2 over a Zn-Deposited Cu(111) Surface, *Surf. Sci.*, 1997, **383**, 285–298.

19 M. Yang, J. Yu, A. Zimina, B. B. Sarma, L. Pandit, J.-D. Grunwaldt, L. Zhang, H. Xu and J. Sun, Probing the Nature of Zinc in Copper-Zinc-Zirconium Catalysts by Operando Spectroscopies for CO_2 Hydrogenation to Methanol, *Angew. Chem., Int. Ed.*, 2023, **62**, e202216803.

20 I. Kasatkin, P. Kurr, B. Kniep, A. Trunschke and R. Schlögl, Role of Lattice Strain and Defects in Copper Particles on the Activity of Cu/ZnO/Al_2O_3 Catalysts for Methanol Synthesis, *Angew. Chem., Int. Ed.*, 2007, **46**, 7324–7327.

21 P. Amann, B. Klötzer, D. Degerman, N. Köpfle, T. Götsch, P. Lömker, C. Rameshan, K. Ploner, D. Bikaljevic, H.-Y. Wang, M. Soldemo, M. Shipilin, C. M. Goodwin, J. Gladh, J. H. Stenlid, M. Börner, C. Schlueter and A. Nilsson, The State of Zinc in Methanol Synthesis Over a Zn/ZnO/Cu(211) Model Catalyst, *Science*, 2022, **376**, 603–608.

22 R. van den Berg, G. Prieto, G. Korpershoek, L. I. van den Wal, A. J. van Bunningen, S. Lægsgaard-Jørgensen, P. E. de Jongh and K. P. de Jong, Structure Sensitivity of Cu and CuZn Catalysts Relevant to Industrial Methanol Synthesis, *Nat. Commun.*, 2016, **7**, 13057.

23 S. D. Pike, A. García-Trenco, E. R. White, A. H. M. Leung, J. Weiner, M. S. P. Shaffer and C. K. Williams, Colloidal Cu/ZnO Catalysts for the Hydrogenation of Carbon Dioxide to Methanol: Investigating Catalyst Preparation and Ligand Effects, *Catal. Sci. Technol.*, 2017, **7**, 3842–3850.

24 M. Zabilskiy, V. L. Sushkevich, D. Palagin, M. A. Newton, F. Krumeich and J. A. van Bokhoven, The Unique Interplay Between Copper and Zinc During Catalytic Carbon Dioxide Hydrogenation to Methanol, *Nat. Commun.*, 2020, **11**, 2409.

25 I. U. Din, M. S. Shaharun, M. A. Alotaibi, A. I. Alharthi and A. Naeem, Recent Developments on Heterogeneous Catalytic CO_2 Reduction to Methanol, *J. CO_2. Util.*, 2019, **34**, 20–33.

26 R. Guil-López, N. Mota, J. Llorente, E. Millán, B. Pawelec, J. L. G. Fierro and R. M. Navarro, Methanol Synthesis from CO_2: A Review of the Latest Developments in Heterogeneous Catalysis, *Materials*, 2019, **12**, 3902.

27 E. A. Romero, T. Zhao, R. Nakano, X. Hu, Y. Wu, R. Jazzar and G. Bertrand, Tandem Copper Hydride-Lewis Pair Catalysed Reduction of Carbon Dioxide into Formate with Dihydrogen, *Nat. Catal.*, 2018, **1**, 743–747.

28 C. M. Wyss, B. K. Tate, J. Bacsa, T. G. Gray and J. P. Sadighi, Bonding and Reactivity of a μ-Hydrido Dicopper Cation, *Angew. Chem., Int. Ed.*, 2013, **52**, 12920–12923.
29 C. M. Zall, J. C. Linehan and A. M. Appel, A Molecular Copper Catalyst for Hydrogenation of CO_2 to Formate, *ACS Catal.*, 2015, **5**, 5301–5305.
30 A. W. Beamer and J. A. Buss, Synthesis, Structural Characterization, and CO_2 Reactivity of a Constitutionally Analogous Series of Tricopper Mono-, Di-, and Trihydrides, *J. Am. Chem. Soc.*, 2023, **145**, 12911–12919.
31 W. Sattler and G. Parkin, Synthesis, Structure, and Reactivity of a Mononuclear Organozinc Hydride Complex: Facile Insertion of CO_2 into a Zn-H Bond and CO_2-Promoted Displacement of Siloxide Ligands, *J. Am. Chem. Soc.*, 2011, **133**, 9708–9711.
32 R. Chambenahalli, A. P. Andrews, F. Ritter, J. Okuda and A. Venugopal, Terminal Hydridozinc Cation, *Chem. Commun.*, 2019, **55**, 2054–2057.
33 R. Chambenahalli, R. M. Bhargav, K. N. McCabe, A. P. Andrews, F. Ritter, J. Okuda, L. Maron and A. Venugopal, Cationic Zinc Hydride Catalyzed Carbon Dioxide Reduction to Formate: Deciphering Elementary Reactions, Isolation of Intermediates, and Computational Investigations, *Chem.–Eur. J.*, 2021, **27**, 7391–7401.
34 N. J. Brown, J. E. Harris, X. Yin, I. Silverwood, A. J. P. White, S. G. Kazarian, K. Hellgardt, M. S. P. Shaffer and C. K. Williams, Mononuclear Phenolate Diamine Zinc Hydride Complexes and Their Reactions with CO_2, *Organometallics*, 2014, **33**, 1112–1119.
35 C. Dong, X. Yang, J. Yao and H. Chen, Mechanistic Study and Ligand Design for the Formation of Zinc Formate Complexes from Zinc Hydride Complexes and Carbon Dioxide, *Organometallics*, 2015, **34**, 121–126.
36 S. P. Cronin, J. M. Strain, M. S. Mashuta, J. M. Spurgeon, R. M. Buchanon and C. A. Grapperhaus, Exploiting Metal-Ligand Cooperativity to Sequester, Activate, and Reduce Atmospheric Carbon Dioxide with a Neutral Zinc Complex, *Inorg. Chem.*, 2020, **59**, 4835–4841.
37 H. Lei, R. Nie, G. Wu and Z. Hou, Hydrogenation of CO_2 to CH_3OH over Cu/ZnO Catalysts with Different ZnO Morphology, *Fuel*, 2015, **154**, 161–166.
38 E. L. Kunkes, F. Studt, F. Abild-Pedersen, R. Schlögl and M. Behrens, Hydrogenation of CO_2 to Methanol and CO on Cu/ZnO/Al_2O_3: Is There a Common Intermediate or Not?, *J. Catal.*, 2015, **328**, 43–48.
39 S. Natesakhawat, J. W. Lekse, J. P. Baltrus, P. R. Ohodnicki Jr, B. H. Howard, X. Deng and C. Matranga, Active Sites and Structure-Activity Relationships of Copper-Based Catalysts for Carbon Dioxide Hydrogenation to Methanol, *ACS Catal.*, 2012, **2**, 1667–1676.
40 C. Bianchini, C. A. Ghilardi, A. Meli, S. Midollini and A. Orlandini, Facile Reduction of Carbon Dioxide, Carbonyl Sulfide, and Carbon Disulfide by Copper(I) Borohydride. X-ray Crystal Structure of the Complex [(triphos)Cu(O_2CH)], *J. Organomet. Chem.*, 1983, **248**, C13–C14.
41 L. Zhang, J. Cheng and Z. Hou, Highly Efficient Catalytic Hydrosilylation of Carbon Dioxide by an *N*-Heterocyclic Carbene Copper Catalyst, *Chem. Commun.*, 2013, **49**, 4782–4784.
42 K. Nakamae, B. Kure, T. Nakajima, Y. Ura and T. Tanase, Facile Insertion of Carbon Dioxide into Cu_2(μ-H) Dinuclear Units Supported by Tetraphosphine Ligands, *Chem.–Asian J.*, 2014, **9**, 3106–3110.
43 E. E. Norwine, J. J. Kiernicki, M. Zeller and N. K. Szymczak, Distinct Reactivity Modes of a Copper Hydride Enabled by an Intramolecular Lewis Acid, *J. Am. Chem. Soc.*, 2022, **144**, 15038–15046.
44 K. Phung, P. Thuéry, J.-C. Berthet and T. Cantat, CO_2/$^{13}CO_2$ Dynamic Exchange in the Formate Complex [(2,9-(^{t}Bu)$_2$-phen)Cu(O_2CH)] and Its Catalytic Activity in the Dehydrogenation of Formic Acid, *Organometallics*, 2023, **42**, 3357–3365.
45 E. A. Patrick, M. E. Bowden, J. D. Erickson, R. M. Bullock and B. L. Tran, Single-Crystal to Single-Crystal Transformations: Stepwise CO_2 Insertions into Bridging Hydrides of $[(NHC)CuH]_2$ Complexes, *Angew. Chem., Int. Ed.*, 2023, **62**, e202304648.
46 G. V. Goeden, J. C. Huffman and K. G. Caulton, A Cu-(μ-H) Bond Can Be Stronger Than an Intramolecular P→Cu Bond. Synthesis and Structure of $Cu_2(\mu\text{-}H)_2[\eta^2\text{-}CH_3C(CH_2PPh_2)_3]_2$, *Inorg. Chem.*, 1986, **25**, 2484–2485.
47 T. Nakajima, Y. Kamiryo, M. Kishimoto, K. Imai, K. Nakamae, Y. Ura and T. Tanase, Synergistic Cu_2 Catalyts for Formic Acid Dehydrogenation, *J. Am. Chem. Soc.*, 2019, **141**, 8732–8736.
48 A. Grasruck, G. Parla, L. Lou, J. Langer, C. Neiß, A. Herrera, S. Frieß, A. Görling, G. Schmid and R. Dorta, Trapping of Soluble, KCl-Stabilized Cu(I) Hydrides with CO_2 gives crystalline formates, *Chem. Commun.*, 2023, **59**, 13879–13882.
49 J. L. Peltier, M. Soleilhavoup, D. Martin, R. Jazzar and G. Bertrand, Absolute Templating of M(111) Cluster Surrogates by Galvanic Exchange, *J. Am. Chem. Soc.*, 2020, **142**, 16479–16485.
50 H. A. Baalbaki, J. Shu, K. Nyamayaro, H.-J. Jung and P. Mehrkhodavandi, Thermally Stable Zinc Hydride Catalyst for Hydrosilylation of CO_2 to Silyl Formate at Atmospheric Pressure, *Chem. Commun.*, 2022, **58**, 6192–6195.
51 W. He, X. Liu and D. Cui, Hydroboration of CO_2 Catalyzed by Heteroscorpionate Zwitterionic Zinc and Magnesium Hydride Complexes, *Dalton Trans.*, 2022, **51**, 4786–4789.
52 F. Ritter, L. J. Morris, K. N. McCabe, T. P. Spaniol, L. Maron and J. Okuda, Deaggregation of Zinc Dihydride by Lewis Acids Including Carbon Dioxide in the Presence of Nitrogen Donors, *Inorg. Chem.*, 2021, **60**, 15583–15592.
53 M. Tüchler, L. Gärtner, S. Fischer, A. D. Boese, F. Belaj and N. C. Mösch-Zanetti, Efficient CO_2 Insertion and Reduction Catalyzed by a Terminal Zinc Hydride Complex, *Angew. Chem., Int. Ed.*, 2018, **57**, 6906–6909.
54 D. M. Ernert, I. Ghiviriga, V. J. Catalano, J. Shearer and L. J. Murray, An Air- and Water-Tolerant Zinc Hydride

Cluster that Reacts Selectively with CO_2, *Angew. Chem., Int. Ed.*, 2015, **54**, 7047–7050.
55 R. Jazzar, M. Soleilhavoup and G. Bertrand, Cyclic (Alkyl)- and (Aryl)-(amino)carbene Coinage Metal Complexes and Their Applications, *Chem. Rev.*, 2020, **120**, 4141–4168.
56 A. J. Jordan, G. Lalic and J. P. Sadighi, Coinage Metal Hydrides: Synthesis, Characterization, and Reactivity, *Chem. Rev.*, 2016, **116**, 8318–8372.
57 T. Nakajima, K. Nakamae, Y. Ura and T. Tanase, Multinuclear Copper Hydride Complexes Supported by Polyphosphine Ligands, *Eur. J. Inorg. Chem.*, 2020, 2211–2226.
58 D. M. Brestensky, D. E. Huseland, C. McGettigan and J. M. Stryker, Simplified, "One-Pot" Procedure for the Synthesis of $[(Ph_3P)CuH]_6$, a Stable Copper Hydride for Conjugate Reductions, *Tetrahedron Lett.*, 1988, **29**, 3749–3752.
59 A. Aloisi, É. Crochet, E. Nicolas, J.-C. Berthet, C. Lescot, P. Thuéry and T. Cantat, Copper-Ligand Cooperativity in H_2 Activation Enables the Synthesis of Copper Hydride Complexes, *Organometallics*, 2021, **40**, 2064–2069.
60 T. Wakamatsu, K. Nagao, H. Ohmiya and M. Sawamura, Copper-Catalyzed Semihydrogenation of Internal Alkynes with Molecular Hydrogen, *Organometallics*, 2016, **35**, 1354–1357.
61 C. M. Zall, J. C. Linehan and A. M. Appel, Triphosphine-Ligated Copper Hydrides for CO_2 Hydrogenation: Structure, Reactivity, and Thermodynamic Studies, *J. Am. Chem. Soc.*, 2016, **138**, 9968–9977.
62 G. V. Goeden and K. G. Caulton, Soluble Copper Hydrides: Solution Behavior and Reactions Related to CO Hydrogenation, *J. Am. Chem. Soc.*, 1981, **103**, 7354–7355.
63 A. E. Nako, Q. W. Tan, A. J. P. White and M. R. Crimmin, Weakly Coordinated Zinc and Aluminum σ-Complexes of Copper(I), *Organometallics*, 2014, **33**, 2685–2688.
64 M. J. Butler and M. R. Crimmin, Magnesium, Zinc, Aluminium and Gallium Hydride Complexes of the Transition Metals, *Chem. Commun.*, 2017, **53**, 1348–1365.
65 E. M. Meyer, S. Gambarotta, C. Floriani, A. Chiesi-Villa and C. Guastini, Polynuclear Aryl Derivatives of Group 11 Metals: Synthesis, Solid State-Solution Structural Relationship, and Reactivity with Phosphines, *Organometallics*, 1989, **8**, 1067–1079.
66 M. Stollenz and F. Meyer, Mesitylcopper - A Powerful Tool in Synthetic Chemistry, *Organometallics*, 2012, **31**, 7708–7727.
67 A. Camus, N. Marsich, G. Nardin and L. Randaccio, A New Type of Stable Organometallic Coper Complex; Properties and Structure of the Product of the Reaction of Arylcopper Compounds with Bis(diphenylphosphino)methane, *J. Organomet. Chem.*, 1973, **60**, C39–C42.
68 K. Nakamae, T. Nakajima, Y. Ura, Y. Kitagawa and T. Tanase, Facially Dispersed Polyhydride Cu_9 and Cu_{16} Clusters Comprising Apex-Truncated Supertetrahedral and Square-Face-Capped Cuboctahedral Copper Frameworks, *Angew. Chem., Int. Ed.*, 2020, **59**, 2262–2267.
69 Q. Tang, Y. Lee, D.-Y. Li, W. Choi, C. W. Liu, D. Lee and D.-e. Jiang, Lattice-Hydride Mechanism in Electrocatalytic CO_2 Reduction by Structurally Precise Copper-Hydride Nanoclusters, *J. Am. Chem. Soc.*, 2017, **139**, 9728–9736.
70 B. Cordero, V. Gómez, A. E. Platero-Prats, M. Revés, J. Echeverría, E. Cremades, F. Barragán and S. Alvarez, Covalent Radii Revisited, *Dalton Trans.*, 2008, 2832–2838.
71 P. Pyykkö and M. Atsumi, Molecular Single-Bond Covalent Radii for Elements 1-118, *Chem.–Eur. J.*, 2008, **15**, 186–197.
72 S. Nag, K. Banerjee and D. Datta, Estimation of the van der Waals Radii of the d-Block Elements Using the Concept of Bond Valence, *New J. Chem.*, 2007, **31**, 832–834.
73 S. S. Batsanov, Van der Waals Radii of Elements, *Inorg. Mater.*, 2001, **37**, 871–885.
74 R. C. Stevens, M. R. McLean and R. Bau, Neutron Diffraction Structure Analysis of a Hexanuclear Copper Hydrido Complex, $H_6Cu_6[P(p\text{-tolyl})_3]_6$: An Unexpected Finding, *J. Am. Chem. Soc.*, 1989, **111**, 3472–3473.
75 E. L. Bennett, P. J. Murphy, S. Imberti and S. F. Parker, Characterization of the Hydrides in Stryker's Reagent: $[HCu\{P(C_6H_5)_3\}]_6$, *Inorg. Chem.*, 2014, **53**, 2963–2967.
76 M. S. Eberhart, J. R. Norton, A. Zuzek, W. Sattler and S. Ruccolo, Electron Transfer from Hexameric Copper Hydrides, *J. Am. Chem. Soc.*, 2013, **135**, 17262–17265.
77 I. Chakraborty and T. Pradeep, Atomically Precise Clusters of Noble Metals: Emerging Link between Atoms and Nanoparticles, *Chem. Rev.*, 2017, **117**, 8208–8271.
78 J. Ko, B.-K. Kim and J. W. Han, Density Functional Theory Study for Catalytic Activation and Dissociation of CO_2 on Bimetallic Alloy Surfaces, *J. Phys. Chem. C*, 2016, **120**, 3438–3447.
79 L.-M. Yang, T. Frauenheim and E. Ganz, Properties of the Free-Standing Two-Dimensional Copper Monolayer, *J. Nanomater.*, 2016, 8429510.
80 A. W. Cook, T.-A. D. Nguyen, W. R. Buratto, G. Wu and T. W. Hayton, Synthesis, Characterization, and Reactivity of the Group 11 Hydrido Clusters $[Ag_6H_4(dppm)_4(OAc)_2]$ and $[Cu_3H(dppm)_3(OAc)_2]$, *Inorg. Chem.*, 2016, **55**, 12435–12440.
81 R. S. Dhayal, J.-H. Liao, Y.-R. Lin, P.-K. Liao, S. Kahlal, J.-Y. Saillard and C. W. Liu, A Nanospheric Polyhydrido Copper Cluster of Elongated Triangular Orthobicupola Array: Liberation of H_2 from Solar Energy, *J. Am. Chem. Soc.*, 2013, **135**, 4704–4707.
82 K. Nakamae, M. Tanaka, B. Kure, T. Nakajima, Y. Ura and T. Tanase, A Fluxional Cu_8H_6 Cluster Supported by Bis(diphenylsphosphino)methane and its Facile Reaction with CO_2, *Chem.–Eur. J.*, 2017, **23**, 9457–9461.
83 A. G. Blackman, E. B. Schenk, R. E. Jelley, E. H. Krenske and L. R. Gahan, Five-Coordinate Transition Metal Complexes and the Value of τ_5: Observations and Caveats, *Dalton Trans.*, 2020, **49**, 14798–14806.
84 A. W. Addison, T. N. Rao, J. Reedijk, J. van Rijn and G. C. Verschoor, Synthesis, Structure and Spectroscopic Properties of Copper(II) Compounds Containing Nitrogen-Sulphur Donor Ligands; the Crystal and Molecular Structure of Aqua[1,7-bis(*N*-methylbenzimidazol-2'-yl)-2,6-dithiaheptane]copper(II) Perchlorate, *J. Chem. Soc., Dalton Trans.*, 1984, 1349–1356.

85 Q. Liu, L. Wu, R. Jackstell and M. Beller, Using Carbon Dioxide as a Building Block in Organic Synthesis, *Nat. Commun.*, 2015, **6**, 5933.
86 T. Ohishi, M. Nishiura and Z. Hou, Carboxylation of Organoboronic Esters Catalyzed by N-Heterocyclic Carbene Copper(I) Complexes, *Angew. Chem., Int. Ed.*, 2008, **47**, 5792–5795.
87 W.-F. Fu, X. Gan, C.-M. Che, Q.-Y. Cao, Z.-Y. Zhou and N. N.-Y. Zhu, Cuprophilic Interactions in Luminescent Copper(I) Clusters with Bridging Bis(dicyclohexylphosphino)methane and Iodide Ligands: Spectroscopic and Structural Investigations, *Chem.–Eur. J.*, 2004, **10**, 2228–2236.
88 Q.-Q. Huang, M.-Y. Hu, Y.-L. Li, N.-N. Chen, Y. Li, Q.-H. Wei and F. Fu, Novel Ultrabright Luminescent Copper Nanoclusters and Application in Light-Emitting Devices, *Chem. Commun.*, 2021, **57**, 9890–9893.
89 C. C. Ho, A. Ariafard, C. J. T. Hyland and A. C. Bissember, Phosphine-Scavenging Cationic Gold(I) Complexes: Alternative Applications of Gold Cocatalysis in Fundamental Palladium-Catalyzed Cross-Couplings, *Organometallics*, 2019, **38**, 2683–2688.
90 E. Wächtler, S. H. Privér, J. Wagler, T. Heine, L. Zhechkov, M. A. Bennett and S. K. Bhargava, Metallophilic Contacts in 2-$C_6F_4PPh_2$ Bridged Heterbinuclear Complexes: A Crystallographic and Computational Study, *Inorg. Chem.*, 2015, **54**, 6947–6957.
91 A. Guerrero, E. Martin, D. L. Hughes, N. Kaltsoyannis and M. Bochmann, Zinc(II) η^1- and η^2-Toluene Complexes: Structure and Bonding in $Zn(C_6F_5)_2\cdot$(toluene) and $Zn(C_6F_4\text{-}2\text{-}C_6F_5)_2\cdot$(toluene), *Organometallics*, 2006, **25**, 3311–3313.
92 J. B. Waters, R. S. P. Turbervill and J. M. Goicoechea, Group 12 Metal Complexes of N-Heterocyclic Ditopic Carbanionic Carbenes, *Organometallics*, 2013, **32**, 5190–5200.
93 C. Borner, L. Anders, K. Brandhorst and C. Kleeberg, Elusive Phosphine Copper(I) Boryl Complexes: Synthesis, Structures, and Reactivity, *Organometallics*, 2017, **36**, 4687–4690.
94 L. L. Cao, K. L. Bamford, L. L. Liu and D. W. Stephan, Zinc-Containing Radical Anions via Single Electron Transfer to Donor-Acceptor Adducts, *Chem.–Eur. J.*, 2018, **24**, 3980–3983.
95 M. H. Chisholm, J. C. Gallucci, H. Yin and H. Zhen, Arylzinc Alkoxides: $[ArZnOChPr^i_2]_2$ and $Ar_2Zn_3(OCHPr^i_2)_4$ When Ar = C_6H_5, *p*-$CF_3C_6H_4$, 2,4,6-$Me_3C_6H_2$, and C_6F_5, *Inorg. Chem.*, 2005, **44**, 4777–4785.
96 P. R. Markies, G. Schat, O. S. Akkerman, F. Bickelhaupt and A. L. Spek, Complexation of Diphenylzinc with Simple Ethers. Crystal Structures of the Complexes $Ph_2Zn\cdot$Glyme and $Ph_2Zn\cdot$Diglyme, *J. Organomet. Chem.*, 1992, **430**, 1–13.
97 D. Specklin, C. Fliedel, C. Gourlaouen, J.-C. Bruyere, T. Avilés, C. Boudon, L. Ruhlmann and S. Dagorne, N-Heterocyclic Carbene Based Tri-organyl-Zn-Alkyl Cations: Synthesis, Structures, and Use in CO_2 Functionalization, *Chem.–Eur. J.*, 2017, **23**, 5509–5519.
98 C. Romain, J. A. Garden, G. Trott, A. Buchard, A. J. P. White and C. K. Williams, Di-Zinc-Aryl Complexes: CO_2 Insertions and Applications in Polymerisation Catalysis, *Chem.–Eur. J.*, 2017, **23**, 7367–7376.
99 S. S. Gholap, M. Takimoto and Z. Hou, Regioselective Alkylative Carboxylation of Allenamides with Carbon Dioxide and Dialkylzinc Reagents Catalyzed by an N-Heterocyclic Carbene-Copper Complex, *Chem.–Eur. J.*, 2016, **22**, 8547–8552.
100 M. Takimoto, S. S. Gholap and Z. Hou, Cu-Catalyzed Alkylative Carboxylation of Ynamides with Dialkylzinc Reagents and Carbon Dioxide, *Chem.–Eur. J.*, 2015, **21**, 15218–15223.
101 M. Takimoto and Z. Hou, Regioselective Carbozincation and Further Functionalization of Allenamides Catalyzed by an *N*-Heterocyclic Carbene (NHC)-Copper Complex, *Asian J. Org. Chem.*, 2023, **12**, e202300372.
102 B. L. Tran, B. D. Neisen, A. L. Speelman, T. Gunasekara, E. S. Wiedner and R. M. Bullock, Mechanistic Studies on the Insertion of Carbonyl Substrates into Cu-H: Different Rate-Limiting Steps as a Function of Electrophilicity, *Angew. Chem., Int. Ed.*, 2020, **59**, 8645–8653.
103 B. M. Zimmermann, T. T. Ngoc, D.-I. Tzaras, T. Kaicharla and J. F. Teichert, A Bifunctional Copper Catalyst Enables Ester Reduction with H_2: Expanding the Reactivity Space of Nucleophilic Copper Hydrides, *J. Am. Chem. Soc.*, 2021, **143**, 16865–16873.
104 J.-X. Chen, J. F. Daeuble, D. M. Brestensky and J. M. Stryker, Highly Chemoselective Catalytic Hydrogenation of Unsaturated Ketones and Aldehydes to Unsaturated Alcohols Using Phosphine-Stabilized Copper(I) Hydride Complexes, *Tetrahedron*, 2000, **56**, 2153–2166.
105 R. Watari, T. Itoh, S. Kuwata and Y. Kayaki, Alkoxide-Decorated Copper Nanoparticles on Amidine-Modified Polymers as Hydrogenation Catalysts for Enabling H_2 Heterolysis, *ACS Catal.*, 2023, **13**, 5169.
106 M. M. D. Roy, A. A. Omaña, A. S. S. Wilson, M. S. Hill, S. Aldridge and E. Rivard, Molecular Main Group Metal Hydrides, *Chem. Rev.*, 2021, **121**, 12784–12965.
107 M. Uchiyama, S. Nakamura, T. Ohwada, M. Nakamura and E. Nakamura, Mechanism and Ligand-Transfer Selectivity of 1,2-Addition of Organozincate Complexes to Aldehyde, *J. Am. Chem. Soc.*, 2004, **126**, 10897–10903.
108 S. D. Robertson, M. Uzelac and R. E. Mulvey, Alkali-Metal-Mediated Synergistic Effects in Polar Main Group Organometallic Chemistry, *Chem. Rev.*, 2019, **119**, 8332–8405.
109 J. M. Parr, A. J. P. White and M. R. Crimmin, Magnesium-Stabilised Transition Metal Formyl Complexes: Structures, Bonding, and Ethenediolate Formation, *Chem. Sci.*, 2022, **13**, 6592–6598.
110 W. Yang, A. J. P. White and M. R. Crimmin, Deoxygenative Coupling of CO with a Tetrametallic Magnesium Hydride Complex, *Angew. Chem., Int. Ed.*, 2024, **63**, e202319626.
111 M. D. Anker, M. S. Hill, J. P. Lowe and M. F. Mahon, Alkaline-Earth-Promoted CO Homologation and

Reductive Catalysis, *Angew. Chem., Int. Ed.*, 2015, **54**, 10009–10011.

112 D. Schuhknecht, T. P. Spaniol, Y. Yang, L. Maron and J. Okuda, Reactivity of a Molecular Calcium Hydride Cation ($[CaH]^+$) Supported by an NNNN Macrocycle, *Inorg. Chem.*, 2020, **59**, 9406–9415.

113 P. Mahawar, T. Rajeshkumar, L. Maron, T. P. Spaniol and J. Okuda, Heterobimetallic Hydrides with a Germanium(II)-Zinc Bond, *Chem.–Eur. J.*, 2023, **29**, e202301496.

114 A. H. M. Leung, A. García-Trenco, A. Phanopoulos, A. Regoutz, M. E. Schuster, S. D. Pike, M. S. P. Shaffer and C. K. Williams, Cu/M:ZnO (M = Mg, Al, Cu) Colloidal Nanocatalysts for the Solution Hydrogenation of Carbon Dioxide to Methanol, *J. Mater. Chem. A*, 2020, **8**, 11282–11291.

115 (*a*) CCDC 2269234: Experimental Crystal Structure, 2025, DOI: **10.5517/ccdc.csd.cc2g5b33**.; (*b*) CCDC 2269235: Experimental Crystal Structure, 2025, DOI: **10.5517/ccdc.csd.cc2g5b44**; (*c*) CCDC 2269236: Experimental Crystal Structure, 2025, DOI: **10.5517/ccdc.csd.cc2g5b55**; (*d*) CCDC 2269237: Experimental Crystal Structure, 2025, DOI: **10.5517/ccdc.csd.cc2g5b66**; (*e*) CCDC 2269238: Experimental Crystal Structure, 2025, DOI: **10.5517/ccdc.csd.cc2g5b77**; (*f*) CCDC 2269239: Experimental Crystal Structure, 2025, DOI: **10.5517/ccdc.csd.cc2g5b88**.